communications physics

ARTICLE

https://doi.org/10.1038/s42005-023-01281-2 OPEN

Emergence of a Bose polaron in a small ring threaded by the Aharonov-Bohm flux

Fabian Brauneis [1✉], Areg Ghazaryan[2], Hans-Werner Hammer [1,3] & Artem G. Volosniev [2✉]

The model of a ring threaded by the Aharonov-Bohm flux underlies our understanding of a coupling between gauge potentials and matter. The typical formulation of the model is based upon a single particle picture, and should be extended when interactions with other particles become relevant. Here, we illustrate such an extension for a particle in an Aharonov-Bohm ring subject to interactions with a weakly interacting Bose gas. We show that the ground state of the system can be described using the Bose-polaron concept—a particle dressed by interactions with a bosonic environment. We connect the energy spectrum to the effective mass of the polaron, and demonstrate how to change currents in the system by tuning boson-particle interactions. Our results suggest the Aharonov-Bohm ring as a platform for studying coherence and few- to many-body crossover of quasi-particles that arise from an impurity immersed in a medium.

[1] Technische Universität Darmstadt, Department of Physics, 64289 Darmstadt, Germany. [2] Institute of Science and Technology Austria (ISTA), Am Campus 1, 3400 Klosterneuburg, Austria. [3] ExtreMe Matter Institute EMMI and Helmholtz Forschungsakademie Hessen für FAIR (HFHF), GSI Helmholtzzentrum für Schwerionenforschung GmbH, 64291 Darmstadt, Germany. ✉email: fbrauneis@theorie.ikp.physik.tu-darmstadt.de; artem.volosniev@ist.ac.at

In the idealized model of a ring threaded by the Aharonov-Bohm (AB) flux, a particle moves in a region with zero fields, and the presence of an electromagnetic potential manifests itself only in a minimal substitution $-i\partial/\partial x \to -i\partial/\partial x + \Phi$, where the position-independent parameter Φ determines the strength of the flux. This model provides insight into many physical phenomena. For example, it illustrates the significance of potentials in quantum mechanics[1], geometric phases[2], the Josephson effect, and persistent currents[3,4]. Foundations of AB physics are based upon a single-particle picture[5,6], which already has the power to explain some experiments qualitatively such as spectroscopy in semiconductor rings[7]. However, one-body studies do not take into account interactions with other particles, in particular, with the environment. Therefore, they should be extended for realistic systems. In this paper, we discuss such an extension assuming a one-dimensional bosonic environment.

Before we proceed, let us briefly review known few-body physics in the AB ring. If all particles are identical, then the flux couples only to the total angular momentum of the system. It can change the global minimum of the energy leaving the internal [i.e., in relative coordinates] dynamics intact, see, e.g.,[6,8–10]. In short, there is no interplay between particle-particle interactions and the AB flux for identical particles. This conclusion holds true also for distinguishable [by spin or quasi-spin] particles with identical masses and AB fluxes. In this case, the strength of the AB flux can however change the symmetry of the ground state, see, e.g., Pecci et al.[11].

For particles with non-identical charges and/or masses, such as electrons and holes[12,13], the internal structure of a one-dimensional system is coupled to the AB flux. At the two-body level, this coupling can modify the threshold for binding (which may preclude formation of excitons for weakly attractive potentials in one dimension[14]) or lead to the formation of dark excitonic states[15]. Systems with more than two particles are less explored, to the best of our knowledge.

In this paper, we study one of the simplest two-component many-body models—a particle (impurity) coupled to the AB flux that interacts with a Bose gas. The system is motivated by recent cold-atom experiments on Bose polarons[16–22], and by theoretical and experimental progress in realizing ring-shape potentials and artificial gauge fields with neutral cold atoms. For reviews of these advances see ref. [23–25]. Ring-shaped condensates with effective gauge potentials have so far not been engineered together with impurities. As we show below such a combination may lead to rich physics. Note that recent advances in engineering ring-shaped potentials[26–28] and tunable gauge fields[29] suggest experiments with polaritons as other set-ups to test our results.

The focus of the paper is on 'dressing' the impurity—a typical question addressed in many-body physics—which determines properties of the system such as transport and 'magnetization'. As such, our results complement previous works that investigated small systems using few-body methods and approaches.

One of the main findings of our work is that the system can be described using ideas developed for the one-dimensional Bose-polaron problem[30–39]. This connection leads to a number of useful conclusions. First, previous studies of the Bose polaron contribute insight into properties of our system, and provide an intuitive interpretation of our results. This insight can be also useful for understanding numerical lattice simulations where electron-phonon interactions are taken into account, see, e.g., Monisha et al.[40]. Second, persistent currents can be an experimental measure of validity of the Bose-polaron concept in one dimension. In particular, they can be used to investigate phase coherence of the polaron across the AB ring—a necessary condition for the existence of persistent currents. Third, the AB ring provides a conceptual model for defining the effective mass in a finite-size system, allowing one to better understand a few- to many-body crossover of one-dimensional systems. In particular, our work paves the way for studying this crossover beyond the standard testbed—the ground-state energy[41].

Results and discussion

System. We study a one-dimensional system of N bosons and a single impurity atom, see Fig. 1. The system is in a ring of length L, which corresponds to periodic boundary conditions. The position of the impurity (ith boson) is given by Ly (Lx_i); the mass of the impurity (a boson) is m (M). We assume that *only* the impurity is coupled to the AB flux Φ/L. For neutral particles, Φ is not generated by a magnetic flux threading the ring. Instead, other techniques are used[23,42], e.g., stirring with a weak external potential with speed v, in which case $\Phi = mvL/\hbar$. Note that the more general case, which might be more suitable for experimental realization, where the artificial flux is coupled to both particle species can be easily incorporated into our model, see Suppl. Note 1 for the flux coupled to bosons.

The Hamiltonian in first quantization reads

$$\mathcal{H} = h + H + V_{ib} + V_{bb}, \tag{1}$$

where $h = \frac{\hbar^2}{2mL^2}\left(-i\partial/\partial y + \Phi\right)^2$ describes the impurity; for the bosons, we have $H = -\frac{\hbar^2}{2ML^2}\sum_i \partial^2/\partial x_i^2$. The impurity-boson, V_{ib}, and boson-boson, V_{bb}, interactions are parameterized by delta-function potentials

$$V_{ib} = \frac{c}{L}\sum_{i=1}^{N}\delta(x_i - y), \quad V_{bb} = \frac{g}{L}\sum_{i,j}\delta(x_i - x_j), \tag{2}$$

where c and g define the strength of interactions. For simplicity, we shall use the system of units in which $\hbar = M = 1$. In the main part of the paper, a boson and the impurity have identical masses, $m = M$. [A mass imbalance does not change the main conclusions of our study, see Suppl. Note 2]. For a fixed value of N, dimensionless parameters that determine all physical properties are c/g and $\gamma = gL/N$. For our numerical simulations, we shall use $\gamma = 0.2$, which corresponds to a weakly interacting Bose gas amenable to the mean-field treatment discussed below. We focus on $c > 0$ to avoid bound states[43–45] that are beyond the polaron physics. Note that the case with $\gamma = 0.2$ and $N = 19$ for $\Phi = 0$ was considered in[46] providing us with a reference point to benchmark our numerical calculations.

In what follows, we shall use the Hamiltonian from Eq. (1) in our analysis. However, it is worthwhile noting that the parameter Φ can in principle be excluded from this Hamiltonian via a gauge transformation $\Psi \to e^{i\Phi y}\Psi$, where Ψ is the wave function. The effect of the flux is then incorporated in a 'twisted' boundary condition that demands that the wave function acquires a phase $e^{i2\pi\Phi}$ after a full turn[47,48]. Such a condition implies that the energy spectrum must be a periodic function with period $\Phi/(2\pi)$ as shown in Fig. 1. Note that for general multi-component systems (e.g, strongly interacting Bose-Fermi mixtures) a smaller period of the ground-state energy is also possible, see, e.g.,[10,11]. As we demonstrate below, this does not happen for an impurity in a weakly-interacting Bose gas whose low-energy spectrum resembles that of a single particle.

The Hamiltonian $\mathcal{H}$ with $\Phi = 0$ corresponds to one of the most studied one-dimensional models[49–52]. Therefore, we can use the already known methods to tackle our problem with $\Phi \neq 0$. We choose to work in the frame co-moving with the impurity (see below), where the mean-field approach (MFA) and flow equations (IM-SRG) provide powerful theoretical tools for our investigation (see Methods). These methods allow us to investigate the effect of the AB flux on the properties of the one-dimensional polaron problem beyond previous studies[53,54],

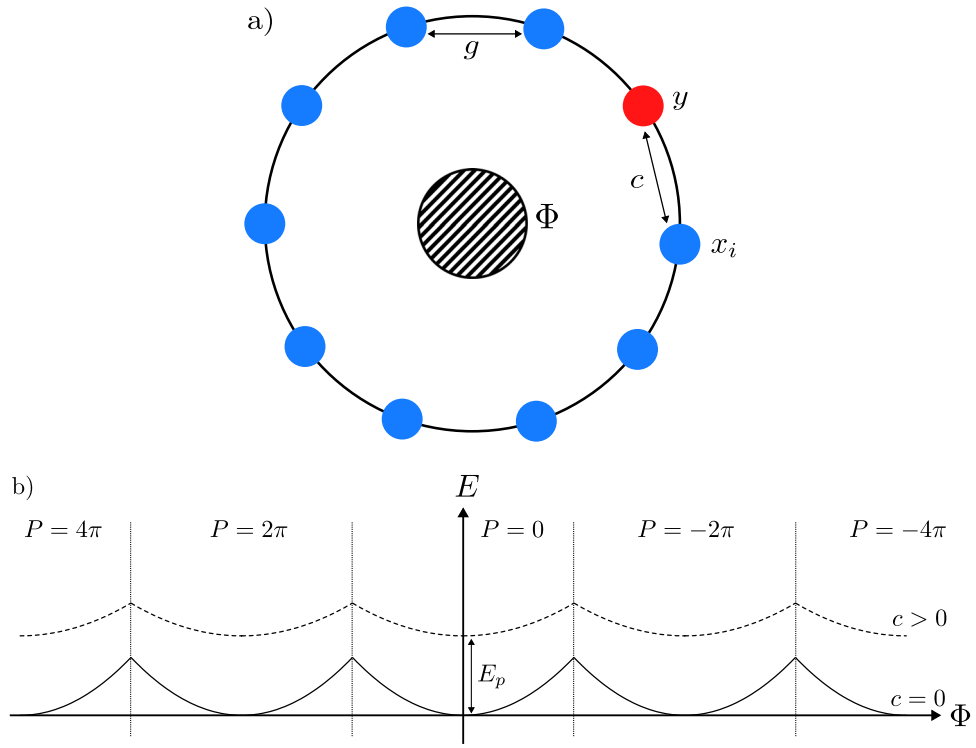

Fig. 1 Sketch of the system and the ground state energy. a Sketch of the system. The bosons are shown as blue balls at the positions x_i; the impurity is a red ball at y. The AB flux is Φ. The strength of the boson-boson (boson-impurity) interaction is given by g (c). **b** Sketch of the ground-state energy as a function of the flux without ($c = 0$) and with ($c > 0$) the interaction with the bosonic environment (leading to an energy shift E_p at $\Phi = 0$). The total momentum of the system is P/L. The shift of the energy spectrum, E_p, and the change of the curvature can be parameterized by effective one-body parameters, see the text for details.

which investigated relevant molecular-crystal models. In particular, we can define and study flux-independent properties of the Bose polaron (e.g., the effective mass) in a finite system.

Co-moving frame. The total momentum of the system is conserved since all interactions are translation-invariant. Therefore, we eliminate the impurity coordinate by writing the wave function as (cf.[55])

$$\Psi(y, \{x_i\}) = \widetilde{\Psi}(\{z_i\})e^{iPy}, \tag{3}$$

where $z_i = \theta(y - x_i) + x_i - y$ [$\theta(x)$ is the Heaviside step function], and P/L is the total momentum. The transformation $\{y, x_i\} \to \{z_i\}$ can be seen as a coordinate-space analog of the Lee-Low-Pines transformation[56]. The parameter P is quantized to fulfill the periodic boundary conditions: $P = 2\pi n$, where n is an integer. Note that the transformation to the co-moving frame has been already used to study the few- to many-body transition in the ground state of the Bose-polaron problem with $\Phi = 0$[35]. Here, we study this transition for non-vanishing P where a continuous parameter Φ provides a bridge between the discrete values of P.

The Schrödinger equation in the co-moving frame reads as follows

$$\left[-\tfrac{1}{2}\left(\sum_i \tfrac{\partial}{\partial z_i}\right)^2 + \tfrac{1}{2}\sum_i \tfrac{\partial^2}{\partial z_i^2} + \tfrac{(P+\Phi)^2}{2} + L^2 V_{ib} + L^2 V_{bb} + i(P+\Phi)\sum_i \tfrac{\partial}{\partial z_i}\right]\widetilde{\Psi} = E\widetilde{\Psi}, \tag{4}$$

where E is the dimensionless energy of the system [to obtain the dimensionful energy one needs to multiply E by $\hbar^2/(mL^2)$]. Note that Φ and P enter this equation together as a sum $\mathcal{P} = P + \Phi$. $\mathcal{P}$ is a continuous variable that can be seen as an effective total momentum that determines total currents in the system. This observation will be crucial for interpreting our results in terms of an effective one-body picture, see below. Note that $\tilde{\Psi}^*_{\mathcal{P}}$ solves the Schrödinger Eq. (4) with $-\mathcal{P}$, which is a manifestation of time-reversal symmetry.

Energy spectrum. The energy spectrum for $\Phi = P = 0$ and finite values of N was calculated in Volosniev et al.[35]. Therefore, in what follows we only calculate $E(P, \Phi) - E(P = 0, \Phi = 0)$, where $E(P, \Phi)$ is the energy of the Hamiltonian for a given value of the total momentum, P, and the AB flux, Φ. $E(P = 0, \Phi = 0)$ approaches the ground-state energy of the Bose-polaron problem in the thermodynamic limit ($N, L \to \infty$ with a fixed value of N/L), see also Suppl. Note 4. Due to the periodicity of the energy (cf. Fig. 1), it is enough to focus on fluxes $-\pi \le \Phi \le \pi$. Furthermore, the energy spectrum is symmetric with respect to $\Phi \to -\Phi$ due to time-reversal symmetry. Therefore, in what follows we shall calculate the lowest-energy states for fixed values of P, so-called Yrast states (cf.[6]), and currents only for $0 \le \Phi \le \pi$. This also fixes the values of the flux needed to observe our findings experimentally.

Energy for $\Phi \neq 0$. We illustrate the energies calculated with MFA and IM-SRG in Fig. 2. For $P = 0$ and $|P| = 2\pi$ both methods agree reasonably well on the energy, demonstrating that the MFA is a useful semi-analytical tool to describe the system. We observed a worse agreement for $|P| \ge 2\pi$. The failure of the mean-field approach is expected for high values of P as there are various ways to distribute momentum between the bosons and the impurity, see also Suppl. Note 3.

Let us give a few general remarks about Fig. 2. For $\Phi = \pm\pi$ there is a level crossing between two Yrast states with $P = 0$ and

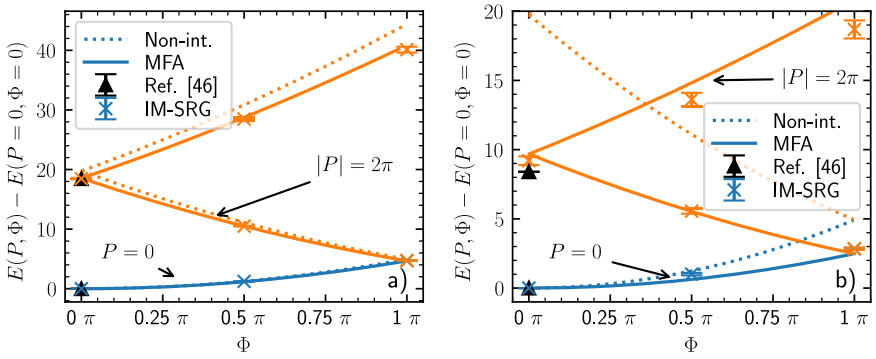

Fig. 2 The energy spectrum as a function of the AB flux, Φ. Different colors correspond to different values of the momentum: Blue $P = 0$ and orange $|P| = 2\pi$. The parameters of the system are $N = 19$, $\gamma = 0.2$, and $c/g = 1$ (**a**), $c/g = 5$ (**b**). The data are obtained using the mean-field ansatz (solid curves, MFA) and the in-medium similarity renormalization group (crosses with errorbars, IM-SRG), black triangles show results from Yang et al.[46] for quantized momenta. The dotted curves show the energy of the non-interacting system.

$|P| = 2\pi$. It is a consequence of the rotational symmetry of the problem. If a defect is introduced into the system, then it will lead to an avoided crossing, see below where we discuss the role of defects. In Fig. 2, we also present the ground-state energy of a non-interacting impurity ($c = 0$), $E = (P + \Phi)^2/2$. We see that the solid curves are always below this value. The effect is more pronounced for stronger impurity-boson interactions—compare the left and right panels of Fig. 2. These features can be easily understood using the concept of a polaron and its effective mass.

Effective mass. For the thermodynamic limit with $\Phi = 0$, one finds that the low-energy spectrum of the system is quadratic in the total momentum (see, e.g.,[39,57] for one-dimensional Bose polarons):

$$\lim_{P\to 0}[E(P,\Phi=0) - E(P=0,\Phi=0)] = \frac{P^2}{2m_{\rm eff}^{\rm TD}}, \qquad (5)$$

where we introduce an effective mass, $m_{\rm eff}^{\rm TD}$; other definitions of the effective mass are discussed in Suppl. Note 5. Eq. (5) is a cornerstone of the polaron concept and effective one-body descriptions of mobile impurities. Note that for small systems, the limit in Eq. (5) should be re-defined since P is discrete.

The parameter Φ is continuous. The mean-field solution as well as time-reversal symmetry suggest that $E(\Phi, P = 0)$ is proportional to Φ^2. By analogy to the Bose-polaron problem, we can define the effective mass of an impurity in a small AB ring

$$\lim_{\Phi\to 0}[E(P=0,\Phi) - E(P=0,\Phi=0)] = \frac{\Phi^2}{2m_{\rm eff}}. \qquad (6)$$

This expression connects our problem to the body of knowledge developed by solving polaron problems. The connection allows one to make predictions about the behavior of an impurity in the AB ring. For example, the effective mass is an increasing function of c. Therefore, one reduces the current associated with the impurity by increasing c, see the discussion below.

In addition, Eq. (6) demonstrates that the AB ring can be a physical testbed for studying the few- to many-body crossover in one-dimensional Bose-polaron problems. We illustrate this crossover for the effective mass in Fig. 3. For weak interactions ($c/g = 0.05$), we see that the effective mass converges to the thermodynamic limit quickly. This is not the case for strong interactions ($c/g = 5$), meaning that many bosons are needed to screen the impurity for large values of c/g. Although, our analysis suggests that the effective mass converges somewhat slower than the energy towards the thermodynamic limit (see also Suppl. Note 4), the basic mechanism is the same: A high compressibility of a weakly-interacting Bose gas requires a large number of bosons to screen a strongly interacting impurity. Note that the number of bosons needed for screening heavily depends on the parameter γ. In particular, in the limit $\gamma \to \infty$, the system fermionizes and the impurity is screened by a handful of particles[41,58,59]. This observation highlights the fact that the few- to many-body crossover should be studied separately for fermions and weakly-interacting bosons.

Finally, we note that the effective mass computed with Eq. (6) describes only the Yrast curve with $P = 0$ well. To illustrate this, we calculate the second derivative of the energy in the limit $\Phi \to 0$ using the MFA. For a non-interacting impurity, this derivative is given by $1/m$ for all values of P. For an interacting impurity, this is not the case. The second derivative for $P = 0$ is by definition given by $1/m_{\rm eff}$. The right panel of Fig. 3 shows that the effective mass increases for stronger impurity-boson repulsion in agreement with our expectations. The figure also shows that for the $|P| = 2\pi$ state additional effects come into play and change the second derivative. The physical picture behind these effects will become more clear below, when we consider currents. The difference between 'effective masses' defined for $P = 0$ and $|P| = 2\pi$ illustrates a shortcoming of the use of the quasiparticle picture for a small AB ring. However, even then, the polaron picture explains the qualitative features of the spectrum well.

Currents. The AB flux in our system induces currents that can be defined via the continuity equations for the impurity and the bosons in the laboratory frame:

$$\frac{\partial\rho_I}{\partial t} = -\frac{\partial j_I}{\partial y}; \quad \frac{\partial\rho_B}{\partial t} = -\frac{\partial j_B}{\partial x}, \qquad (7)$$

where tL^2 is time, ρ_I (ρ_B) is the probability density of the impurity (bosonic) cloud. The (local) probability currents are defined as

$$j_I = -\frac{i}{2}\int {\rm d}x_1 \ldots {\rm d}x_N \left(\Psi^* \frac{\partial\Psi}{\partial y} - \Psi\frac{\partial\Psi^*}{\partial y}\right) + \Phi\rho_I, \qquad (8)$$

$$j_B = -\frac{i}{2}\int {\rm d}y{\rm d}x_2 \ldots {\rm d}x_N \left(\Psi^* \frac{\partial\Psi}{\partial x_1} - \Psi\frac{\partial\Psi^*}{\partial x_1}\right). \qquad (9)$$

The rotational symmetry implies that j_I, j_B, ρ_I and ρ_B are position-independent, allowing us to work with the integral quantities, e.g., $\rho_I = \int\rho_I {\rm d}y/(2\pi)$, which is more convenient. For example, using these quantities, it is easy to show that $j_I + Nj_B = \mathcal{P}$. Therefore, the total current—the current that corresponds to the total density $\rho_I + N\rho_B$—is given by $\mathcal{P} = P + \Phi$. Note that even though the AB flux is coupled only to the impurity, boson-impurity interactions also generate a current of bosons. We illustrate these currents for $c/g = 1$ and

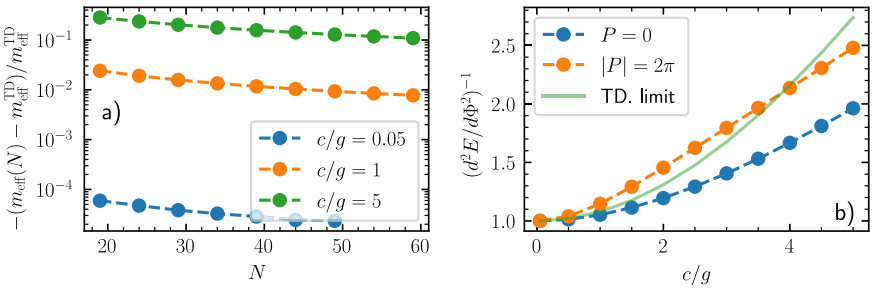

Fig. 3 Effective mass for a finite-size system. a Convergence of the effective mass to its thermodynamic limit for $\gamma = 0.2$ and different values of c/g. **b** Inverse of $\frac{d^2E}{d\Phi^2}$ for $\Phi \to 0$ with $P = 0$ and $|P| = 2\pi$. The parameters of the system are $N = 19$, $\gamma = 0.2$. The green curve shows the known result for $P \to 0$ in the thermodynamic limit (TD. limit)[39, 57]. The data in both panels are obtained using the mean-field approach.

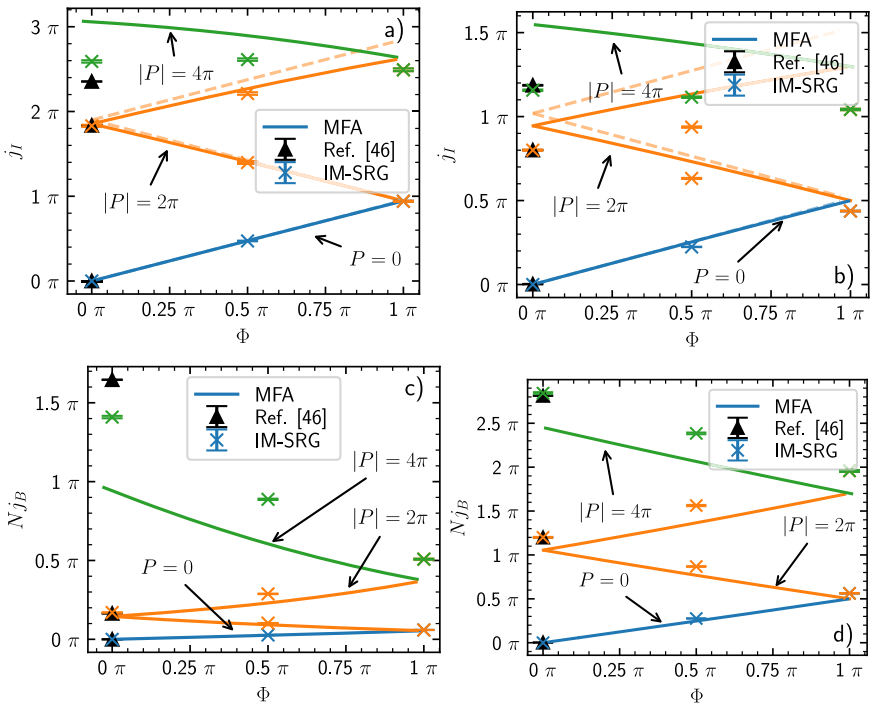

Fig. 4 Currents in the system. a, **b** present the impurity current. **c**, **d** demonstrate the bosonic current. Blue, orange, and green colors are for $P = 0$, $|P| = 2\pi$, and $|P| = 4\pi$, correspondingly. The parameters of the system are $N = 19$ and $\gamma = 0.2$. **a**, **c** show results for $c/g = 1$, whereas **b**, **d** are for $c/g = 5$. Data were obtained with the mean-field ansatz (solid lines, MFA) and in-medium similarity renormalization group (crosses, IM-SRG). Black triangles are the results of Yang et al.[46] for $\Phi = 0$. Dashed lines in **a**, **c** show the impurity current in the polaron approximation $j_I = \mathcal{P}/m_{\text{eff}}$. Here, m_{eff} is calculated within the MFA using Eq. (6).

$c/g = 5$ in Fig. 4 (other parameters are $N = 19$, $\gamma = 0.2$). The increase in the boson-impurity interaction leads to an increase in the bosonic current. This observation is most easily explained using the Bose-polaron picture.

Using the Hellmann-Feynman theorem, it is straightforward to show that

$$j_I = \frac{\partial E}{\partial \Phi}, \tag{10}$$

which coincides with the standard definition of the current in a one-body problem, see, e.g.,[6]. [Note that this expression provides an indirect way for measuring currents by studying the energy landscape of the problem with RF spectroscopy (cf. Scazza et al. [60]).] For the polaron picture with $P = 0$, this leads to $j_I = \Phi/m_{\text{eff}}$ connecting the current (and transport properties) of the impurity to its effective mass. The bosonic current in the same approximation is given by $Nj_B = (1 - 1/m_{\text{eff}})\Phi$. The bosonic current generated by the AB flux follows the impurity, and leads to renormalization of its mass. We conclude that in the polaron picture the currents depend linearly on Φ, with the slope fully determined by the effective mass.

The region of validity of this picture is determined by the boson-impurity interaction, see the dashed lines in panels a) and b) of Fig. 4. For $c/g = 1$ we observe that the polaron approximation, in which the energy is related to the AB flux via Eq. (6), is accurate for $|\mathcal{P}| \lesssim 2\pi$, but for stronger interactions, $c/g = 5$, it is appropriate merely for $|\mathcal{P}| \lesssim \pi$. For even stronger interactions, Eq. (6) is accurate only in the limit $\mathcal{P} \to 0$. Our interpretation here is that the coherent propagation of the impurity is not possible for strong boson-impurity interaction and large fluxes. Indeed, for $c \to \infty$ the impurity can exchange its position with a boson in a coherent manner only at timescales given by $1/c$. Thus strong (fast) impurity currents excite bosons. This leads to a non-linear increase of the currents with Φ, see also ref. [46] and Suppl. Note 3. To quantify these effects, it is convenient to rely on the second derivative of the energy (effective mass), which is larger for $|P| = 2\pi$, see Fig. 3 (note that the bosonic current is related to the impurity current via $Nj_B = P + \Phi - j_I$, i.e., one can reach the same conclusion by

considering Nj_B instead of j_I). The IM-SRG results show a somewhat stronger generation of bosonic currents than the MFA, but the qualitative picture stays the same.

In addition limits of validity of the polaron picture can be investigated by considering states with higher values of $|P|$. For example, Fig. 4 shows that for $|P| = 4\pi$, the current of the impurity (almost) does not depend on Φ. This current is critical in a sense that by changing the flux of the impurity one generates only the current of bosons. The value of the critical current, j_I^{cr}, is decreased by increasing c, in agreement with the mean-field studies[61,62].

The critical current can be seen as an analog of the critical velocity of a classic impurity that moves in a superfluid (cf. Landau critical velocity). Using this analogy, we can understand why the mean-field approximation in the co-rotating frame does not provide the correct value of the critical current. The MFA does not describe accurately the excitations of the Bose gas when it is decoupled from the impurity. In particular, the MFA leads to an incorrect phononic dispersion relation and implies that the critical velocity can be larger than the speed of sound for small values of c/g[62], which is unphysical. Furthermore, it does not capture type-II excitations of the Lieb-Liniger gas[63], which define the lowest energy state for a given value of the momentum of the Bose gas, see[64] for tutorial. Note that our IM-SRG method also does not capture these states well—the flow equations diverge when the type-II excitations become relevant. For some additional details, see Suppl. Note 3.

Role of defects. The rotational symmetry of the problem makes the Yrast energy spectrum of Fig. 2 double degenerate at $\Phi = \pm\pi$. In realistic systems, the symmetry is typically broken due to the presence of defects, leading to avoided crossings in the energy spectrum (cf. Fig. 5). At the maxima of the avoided crossings one-body currents defined via $\partial E/\partial\Phi$ vanish affecting transport properties of the system[5]. We also note that the simplest experimental realization of the AB flux in cold-atom set-ups can be achieved with a rotating weak link[65], which utilizes the equivalence between the Coriolis force in a non-inertial frame and the Lorentz force on a charged particle in a uniform magnetic field. The rotating link introduces a 'defect' potential into the problem whose effect can be studied using the methods discussed in this section.

Our two-component set-up offers unique possibilities to modify currents that are not present in single-body AB physics. To illustrate this, we add to the Hamiltonian a small perturbation:

$$\mathcal{H}_W = \mathcal{H} + W, \tag{11}$$

where $\mathcal{H}$ is the original Hamiltonian from Eq. (1) and

$$W = \frac{a}{L}\sum_i \delta(x_i). \tag{12}$$

This additional term describes a short-range potential coupled *exclusively* to the Bose gas. The current of the impurity is sensitive to W only via the boson-impurity interaction, and therefore the avoided crossing should contain information about the boson-impurity correlation function.

As long as a is small ($a \to 0$), we can assume that the defect has only a minor influence on our system unless the system is close to the degeneracy point, $\Phi = \pm\pi$. Close to these points, we calculate the dimensionless energy using degenerate state perturbation theory:

$$\mathcal{H}_W \simeq \begin{pmatrix} E_0 + L^2\langle\Psi_0|W|\Psi_0\rangle & L^2\langle\Psi_0|W|\Psi_1\rangle \\ L^2\langle\Psi_1|W|\Psi_0\rangle & E_1 + L^2\langle\Psi_1|W|\Psi_1\rangle \end{pmatrix},$$

where $E_0 \simeq \Phi^2/(2m_{\rm eff})$ ($E_1 \simeq \Phi^2/(2m_{\rm eff})$) is the energy of the Yrast state with $P = 0$ ($|P| = 2\pi$); Ψ_0 (Ψ_1) is the corresponding eigenstate. Within the MFA, the matrix elements read as

$$\langle\Psi_i|W|\Psi_j\rangle = \frac{a}{L}N\alpha^{N-1}\int e^{i(P_j-P_i)y} f_i^*(y) f_j(y)dy,$$

where $\alpha = \int f_i^*(z) f_j(z)dz$, and subscripts determine the Yrast state, e.g., $i = 0$ corresponds to $P = 0$.

To provide insight into the avoided crossing, we focus on $\Phi = \pm\pi$. In this case $f_1 = f_0$, and $\langle\Psi_i|W|\Psi_j\rangle$ depends only on the density in the co-moving frame (or equivalently on the impurity-boson correlation function in the laboratory frame). This density, hence, the splitting of the energy levels, is sensitive to the values of c. For example, if $c = 0$, then the defect should destroy the rotational invariance of the Bose gas only. Indeed, in this case, $|f|^2$ is constant and $\langle\Psi_i|W|\Psi_j\rangle = 0$.

Panel a) of Fig. 5 illustrates the avoided crossing for a small value of a. Note that the energy of the system, $E(P, \Phi)$, increases for $a > 0$. This effect does not appear in the figure as we only show the energy difference. The interesting part is that in the presence of W the energies of the first and second Yrast state no longer cross. The splitting of the energies, $\Delta E = 2aLNI$, is determined by the integral

$$I = \int e^{i2\pi y}|f_0(y)|^2 dy, \tag{13}$$

which can be estimated using the density in the thermodynamic limit at $\Phi = 0$[66]:

$$|f_0(y)|^2 \simeq \frac{L\mu}{g(N-1)}\tanh^2\left(\sqrt{\mu\kappa}L\delta\left[\frac{(z-L/2)}{\delta L} + \frac{1}{2}\right]\right),$$

where

$$\delta \simeq 1 + \frac{2d}{\sqrt{\gamma\kappa}N}, \quad d = \frac{1}{2}\,\mathrm{asinh}\left(\frac{2\rho}{c}\sqrt{\frac{\gamma}{\kappa}}\right), \tag{14}$$

$$\mu \simeq \gamma\rho^2\frac{N-1}{N}\left(1 - 2\frac{\tanh(d) - 1}{\sqrt{\gamma\kappa}N}\right). \tag{15}$$

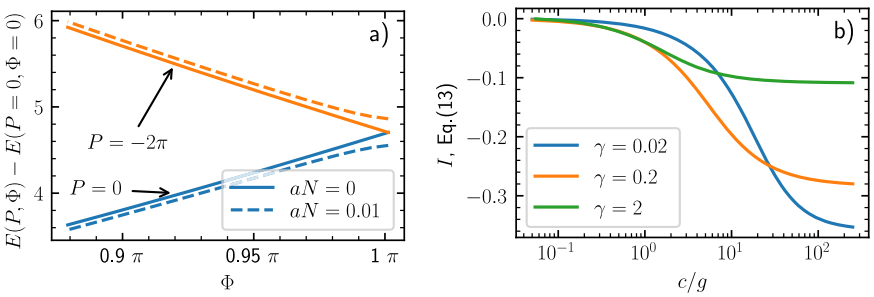

Fig. 5 Effect of a defect on the energy crossing. a The energy for $P = 0$ and $P = -2\pi$ as a function of the flux with and without a defect. Solid lines are for the unperturbed system; dashed lines correspond to $aN = 0.01$. Other parameters of the system are $N = 19$, $\gamma = 0.2$, and $c/g = 1$. **b** Eq. (13) in the thermodynamic limit as a function of c/g for different boson-boson interactions γ. The data were obtained with the mean-field ansatz.

Panel b) of Fig. 5 shows that by increasing the value of c, one increases the energy splitting. Since the interactions are of zero range, the value of I converges to a constant value for $c \to \infty$, which depends on the strength of boson-boson interactions, γ. Note that for small values of γ the impurity can modify the density of the bosons significantly, leading to larger values of I.

Finally, we note an interference effect that appears if we place a second small perturbation into the system:

$$W = \frac{a}{L}\sum_i \big(\delta(x_i) + \delta(x_i + d)\big). \tag{16}$$

In analogy to above, we can define a coupling integral as

$$I = \left(1 + e^{i2\pi d}\right) \int e^{i2\pi y} |f_0(y)|^2 \mathrm{d}y. \tag{17}$$

If $d = 1/2$, this matrix element vanishes and the energy levels cross again (within the lowest order of perturbation theory). This happens because the perturbations are placed opposite to one another, which effectively restores the rotational symmetry in this case. This effect can be seen also for more than two perturbations, as long as they are placed in a symmetric order on the ring (for example three defects in a form of an equilateral triangle).

Conclusions

To summarize, we studied an impurity coupled to the AB flux in a Bose gas. We argued that (i) the system can be described using the ideas developed for the Bose polaron, (ii) the AB ring can be a testbed for studies of the few- to many-body crossover in cold-atom polaron problems. In particular, observation of persistent currents in the AB ring with an impurity can shed light onto coherence properties of the Bose polaron. Note that the 1D world has inherent phase fluctuations, which can be captured using the IM-SRG approach (see also Suppl. Note 3). These fluctuations should be necessarily taken into account when studying persistent currents of polarons.

Our investigation of currents shows that the AB ring can provide a platform for studying a few-body analog of the critical velocity in a Bose-polaron problem. Furthermore, if we assume that the critical current, j_I^{cr}, does not depend on Φ, then (according to Eq. (10)) the energy of the system is $E = E^{cr} + j_I^{cr}\Phi$. This expression connects the bosonic current and the energy of the system motivating a study of few-body precursors of collective excitations in a Bose gas.

Finally, we note that $\partial^2 E/(\partial\Phi^2)$ relates to the inverse of the effective mass, which defines transport properties of a polaron. This relation bears some similarity to the Thouless conductance in a disordered medium[67]. It might be interesting to explore this connection further, in particular, for a weakly interacting light impurity that within the Born-Oppenheimer approximation experiences a disorder potential created by heavy bosons.

Methods

Mean-field approach. We use two methods to investigate the system. The first one is the mean-field approach (MFA) in relative coordinates. It assumes that all bosons occupy one state in the frame co-moving with the impurity, so that the total wave function of the system can be approximated as

$$\widetilde{\Psi}(z_1, z_2, \ldots, z_N) = \prod_{i=1}^{N} f(z_i), \tag{18}$$

where $f(z)$ is a normalized function determined by minimizing the Hamiltonian. The variational procedure leads to the Gross-Pitaevskii equation, which can be solved semi-analytically, see Cominotti et al.[68] and Suppl. Note 3.

Flow equations. The MFA is a well-established approach by now whose accuracy for stationary impurity problems has been shown by comparing to numerical quantum Monte Carlo[35,69] and state-of-the-art RG methods[35,39,68,70]. The MFA in time-dependent problems was discussed in[71,72]. In spite of those previous tests of MFA, we still find it necessary to validate it for the problem at hand. To this end, we shall use flow equations in the form of the so-called in-medium similarity renormalization group method (IM-SRG). This is an ab initio method that has been employed in condensed matter and nuclear physics[73–75] (for applications for one-dimensional problems with impurities, see ref. [35,45,70]). For convenience of the reader, we provide a brief introduction into IM-SRG and further compare its results to the MFA in Suppl. Note 3.

Data availability

The data that support the findings of this study are available from the corresponding author upon reasonable request.

Code availability

The code used for this study is available from the corresponding author upon reasonable request.

Received: 8 February 2023; Accepted: 21 June 2023;
Published online: 22 August 2023

References

1. Aharonov, Y. & Bohm, D. Significance of electromagnetic potentials in the quantum theory. *Phys. Rev.* **115**, 485–491 (1959).
2. Berry, M. V. Quantal phase factors accompanying adiabatic changes. *Proc. R. Soc. Lond. A. Math. Phys. Sci.* **392**, 45–57 (1984).
3. Bloch, F. Simple interpretation of the Josephson effect. *Phys. Rev. Lett.* **21**, 1241–1243 (1968).
4. Büttiker, M., Imry, Y. & Landauer, R. Josephson behavior in small normal one-dimensional rings. *Phys. Lett. A* **96**, 365–367 (1983).
5. Aronov, A. G. & Sharvin, Y. V. Magnetic flux effects in disordered conductors. *Rev. Mod. Phys.* **59**, 755–779 (1987).
6. Viefers, S., Koskinen, P., Singha Deo, P. & Manninen, M. Quantum rings for beginners: energy spectra and persistent currents. *Phys. E: Low.-Dimens. Syst. Nanostruct.* **21**, 1–35 (2004).
7. Lorke, A. et al. Spectroscopy of nanoscopic semiconductor rings. *Phys. Rev. Lett.* **84**, 2223–2226 (2000).
8. Müller-Groeling, A., Weidenmüller, H. A. & Lewenkopf, C. H. Interacting electrons in mesoscopic rings. *Europhys. Lett.* **22**, 193 (1993).
9. Manninen, M., Viefers, S. & Reimann, S. Quantum rings for beginners ii: Bosons versus fermions. *Phys. E: Low.-Dimens. Syst. Nanostruct.* **46**, 119–132 (2012).
10. Naldesi, P. et al. Enhancing sensitivity to rotations with quantum solitonic currents. *SciPost Phys.* **12**, 138 (2022).
11. Pecci, G., Aupetit-Diallo, G., Albert, M., Vignolo, P. & Minguzzi, A. Persistent currents in a strongly interacting multicomponent Bose gas on a ring. https://arxiv.org/abs/2211.16194 (2022).
12. Römer, R. A. & Raikh, M. E. Aharonov-Bohm effect for an exciton. *Phys. Rev. B* **62**, 7045–7049 (2000).
13. Kyriakou, K., Moulopoulos, K., Ghazaryan, A. V. & Djotyan, A. P. Arbitrary mixture of two charged interacting particles in a magnetic Aharonov-Bohm ring: persistent currents and Berry's phases. *J. Phys. A: Math. Theor.* **43**, 354018 (2010).
14. Moulopoulos, K. & Constantinou, M. Two interacting charged particles in an Aharonov-Bohm ring: bound state transitions, symmetry breaking, persistent currents, and Berry's phase. *Phys. Rev. B* **70**, 235327 (2004).
15. Ghazaryan, A. V., Djotyan, A. P., Moulopoulos, K. & Kirakosyan, A. A. Linear dynamic polarizability and the absorption spectrum of an exciton in a quantum ring in a magnetic field. *Phys. Scr.* **83**, 035703 (2011).
16. Spethmann, N. et al. Dynamics of single neutral impurity atoms immersed in an ultracold gas. *Phys. Rev. Lett.* **109**, 235301 (2012).
17. Catani, J. et al. Quantum dynamics of impurities in a one-dimensional Bose gas. *Phys. Rev. A* **85**, 023623 (2012).
18. Hu, M.-G. et al. Bose Polarons in the Strongly Interacting Regime. *Phys. Rev. Lett.* **117**, 055301 (2016).
19. Jørgensen, N. B. et al. Observation of attractive and repulsive polarons in a Bose-Einstein condensate. *Phys. Rev. Lett.* **117**, 055302 (2016).
20. Peña Ardila, L. A. et al. Analyzing a Bose polaron across resonant interactions. *Phys. Rev. A* **99**, 063607 (2019).
21. Yan, Z. Z., Ni, Y., Robens, C. & Zwierlein, M. W. Bose polarons near quantum criticality. *Science* **368**, 190–194 (2020).
22. Skou, M. G. et al. Non-equilibrium quantum dynamics and formation of the Bose polaron. *Nat. Phys.* **17**, 731–735 (2021).
23. Dalibard, J., Gerbier, F., Juzeliūnas, G. & Öhberg, P. Colloquium: Artificial gauge potentials for neutral atoms. *Rev. Mod. Phys.* **83**, 1523–1543 (2011).
24. Amico, L. et al. Roadmap on atomtronics: state of the art and perspective. *AVS Quantum Sci.* **3**, 039201 (2021).

25. Amico, L. et al. Colloquium: Atomtronic circuits: From many-body physics to quantum technologies. *Rev. Mod. Phys.* **94** https://doi.org/10.1103/revmodphys.94.041001. (2022).
26. Aladinskaia, E. et al. Spatial quantization of exciton-polariton condensates in optically induced traps. *Phys. Rev. B* **107**, 045302 (2023).
27. Lukoshkin, V. A. et al. Persistent circular currents of exciton-polaritons in cylindrical pillar microcavities. *Phys. Rev. B* **97**, 195149 (2018).
28. Kalevich, V. et al. Ring-shaped polariton lasing in pillar microcavities. *J. Appl. Phys.* **115**, 094304 (2014).
29. Lim, H.-T., Togan, E., Kroner, M., Miguel-Sanchez, J. & Imamoğlu, A. Electrically tunable artificial gauge potential for polaritons. *Nat. Commun.* **8**, 14540 (2017).
30. Casteels, W., Tempere, J. & Devreese, J. T. Polaronic properties of an impurity in a Bose-Einstein condensate in reduced dimensions. *Phys. Rev. A* **86**, 043614 (2012).
31. Petković, A. & Ristivojevic, Z. Dynamics of a mobile impurity in a one-dimensional Bose liquid. *Phys. Rev. Lett.* **117**, 105301 (2016).
32. Schecter, M., Gangardt, D. M. & Kamenev, A. Quantum impurities: from mobile Josephson junctions to depletons. *N. J. Phys.* **18**, 065002 (2016).
33. Parisi, L. & Giorgini, S. Quantum Monte Carlo study of the Bose-polaron problem in a one-dimensional gas with contact interactions. *Phys. Rev. A* **95**, 023619 (2017).
34. Grusdt, F., Astrakharchik, G. E. & Demler, E. Bose polarons in ultracold atoms in one dimension: beyond the Fröhlich paradigm. *N. J. Phys.* **19**, 103035 (2017).
35. Volosniev, A. G. & Hammer, H.-W. Analytical approach to the Bose-polaron problem in one dimension. *Phys. Rev. A* **96**, 031601 (2017).
36. Pastukhov, V. Impurity states in the one-dimensional Bose gas. *Phys. Rev. A* **96**, 043625 (2017).
37. Kain, B. & Ling, H. Y. Analytical study of static beyond-Fröhlich Bose polarons in one dimension. *Phys. Rev. A* **98**, 033610 (2018).
38. Mistakidis, S. I., Katsimiga, G. C., Koutentakis, G. M., Busch, T. & Schmelcher, P. Quench dynamics and orthogonality catastrophe of bose polarons. *Phys. Rev. Lett.* **122**, 183001 (2019).
39. Jager, J., Barnett, R., Will, M. & Fleischhauer, M. Strong-coupling Bose polarons in one dimension: condensate deformation and modified Bogoliubov phonons. *Phys. Rev. Res.* **2**, 033142 (2020).
40. Monisha, P., Sankar, I., Sil, S. & Chatterjee, A. Persistent current in a correlated quantum ring with electron-phonon interaction in the presence of Rashba interaction and Aharonov-Bohm flux. *Sci. Rep.* **6**, 20056 (2016).
41. Wenz, A. et al. From few to many: Observing the formation of a Fermi sea one atom at a time. *Science* **342**, 457–460 (2013).
42. Goldman, N., Juzeliūnas, G., Öhberg, P. & Spielman, I. B. Light-induced gauge fields for ultracold atoms. *Rep. Prog. Phys.* **77**, 126401 (2014).
43. Gunn, J. C. & Gunn, J. M. F. An exactly soluble hartree problem in an external potential. *Eur. J. Phys.* **9**, 51 (1988).
44. Kolomeisky, E. B., Straley, J. P. & Kalas, R. M. Ground-state properties of artificial bosonic atoms, Bose interaction blockade, and the single-atom pipette. *Phys. Rev. A* **69**, 063401 (2004).
45. Brauneis, F. et al. Artificial atoms from cold bosons in one dimension. *N. J. Phys.* **24**, 063036 (2022).
46. Yang, M., C¨ufar, M., Pahl, E. & Brand, J. Polaron-depleton transition in the yrast excitations of a one-dimensional Bose gas with a mobile impurity. *Condens. Matter* **7**, 15 (2022).
47. Byers, N. & Yang, C. N. Theoretical considerations concerning quantized magnetic flux in superconducting cylinders. *Phys. Rev. Lett.* **7**, 46–49 (1961).
48. Imry, Y. Physics of mesoscopic systems, 101–163. https://www.worldscientific.com/doi/abs/10.1142/9789814415309_0004 (1986).
49. Cazalilla, M. A., Citro, R., Giamarchi, T., Orignac, E. & Rigol, M. One dimensional bosons: from condensed matter systems to ultracold gases. *Rev. Mod. Phys.* **83**, 1405–1466 (2011).
50. Guan, X.-W., Batchelor, M. T. & Lee, C. Fermi gases in one dimension: from Bethe ansatz to experiments. *Rev. Mod. Phys.* **85**, 1633–1691 (2013).
51. Sowiński, T. & García-March, M. Á. One-dimensional mixtures of several ultracold atoms: a review. *Rep. Prog. Phys.* **82**, 104401 (2019).
52. Mistakidis, S. I. et al. Cold atoms in low dimensions—a laboratory for quantum dynamics. https://arxiv.org/abs/2202.11071 (2022).
53. Chen, H. & Chen, Y. Influence of the Aharonov-Bohm flux on the optical polarons in the molecular-crystal model with the dispersion term in a ring. *Solid State Commun.* **105**, 537–541 (1998).
54. Zhou, Y.-C., Chen, H. & Yu, C.-F. Effect of the Aharonov-Bohm potential on the acoustical polaron in one-dimensional rings. *Phys. Lett. A* **212**, 167–170 (1996).
55. Gross, E. Motion of foreign bodies in boson systems. *Ann. Phys.* **19**, 234–253 (1962).
56. Lee, T. D., Low, F. E. & Pines, D. The motion of slow electrons in a polar crystal. *Phys. Rev.* **90**, 297–302 (1953).
57. Mistakidis, S. I., Volosniev, A. G., Zinner, N. T. & Schmelcher, P. Effective approach to impurity dynamics in one-dimensional trapped Bose gases. *Phys. Rev. A* **100**, 013619 (2019).
58. Astrakharchik, G. E. & Brouzos, I. Trapped one-dimensional ideal Fermi gas with a single impurity. *Phys. Rev. A* **88**, 021602 (2013).
59. Levinsen, J., Massignan, P., Bruun, G. M. & Parish, M. M. Strong-coupling ansatz for the one-dimensional Fermi gas in a harmonic potential. *Sci. Adv.* **1**, 6 (2015).
60. Scazza, F. et al. Repulsive Fermi polarons in a resonant mixture of ultracold ^{6}Li atoms. *Phys. Rev. Lett.* **118**, 083602 (2017).
61. Hakim, V. Nonlinear schrödinger flow past an obstacle in one dimension. *Phys. Rev. E* **55**, 2835–2845 (1997).
62. Smith, D. H. & Volosniev, A. G. Engineering momentum profiles of cold-atom beams. *Phys. Rev. A* **100**, 033604 (2019).
63. Lieb, E. H. Exact analysis of an interacting Bose gas. ii. the excitation spectrum. *Phys. Rev.* **130**, 1616–1624 (1963).
64. Syrwid, A. Quantum dark solitons in ultracold one-dimensional Bose and Fermi gases. *J. Phys. B: At. Mol. Opt. Phys.* **54**, 103001 (2021).
65. Wright, K. C., Blakestad, R. B., Lobb, C. J., Phillips, W. D. & Campbell, G. K. Driving phase slips in a superfluid atom circuit with a rotating weak link. *Phys. Rev. Lett.* **110**, 025302 (2013).
66. Volosniev, A. G. & Hammer, H.-W. Flow equations for cold Bose gases. *N. J. Phys.* **19**, 113051 (2017).
67. Thouless, D. Electrons in disordered systems and the theory of localization. *Phys. Rep.* **13**, 93–142 (1974).
68. Cominotti, M., Rossini, D., Rizzi, M., Hekking, F. & Minguzzi, A. Optimal persistent currents for interacting bosons on a ring with a gauge field. *Phys. Rev. Lett.* **113**, 025301 (2014).
69. Panochko, G. & Pastukhov, V. Mean-field construction for spectrum of one-dimensional Bose polaron. *Ann. Phys.* **409**, 167933 (2019).
70. Brauneis, F., Hammer, H.-W., Lemeshko, M. & Volosniev, A. G. Impurities in a one-dimensional Bose gas: the flow equation approach. *SciPost Phys.* **11**, 008 (2021).
71. Jager, J. & Barnett, R. Stochastic-field approach to the quench dynamics of the one-dimensional Bose polaron. *Phys. Rev. Res.* **3**, 033212 (2021).
72. Koutentakis, G. M., Mistakidis, S. I. & Schmelcher, P. Pattern formation in one-dimensional polaron systems and temporal orthogonality catastrophe. *Atoms* **10**, 3 (2022).
73. Kehrein, S. The Flow Equation Approach to Many-Particle Systems (Springer, Berlin, 2006).
74. Tsukiyama, K., Bogner, S. K. & Schwenk, A. In-medium similarity renormalization group for nuclei. *Phys. Rev. Lett.* **106**, 222502 (2011).
75. Hergert, H., Bogner, S., Morris, T., Schwenk, A. & Tsukiyama, K. The in-medium similarity renormalization group: a novel ab initio method for nuclei. *Phys. Rep.* **621**, 165–222 (2016).

Acknowledgements

We would like to thank Jonas Jager for sharing his data with us in the early stages of this project. We thank Joachim Brand and Ray Yang for sharing with us data from Yang et al.[46]. This work has received funding from the DFG Project no. 413495248 [VO 2437/1-1] (F.B., H.-W.H., A.G.V.). We acknowledge support from the Deutsche Forschungsgemeinschaft (DFG - German Research Foundation) and the Open Access Publishing Fund of the Technical University of Darmstadt.

Author contributions

A.G.V. and F.B. designed the project; F.B. performed calculations under the supervision of A.G.V. and H.-W.H; F.B., A.G., H.-W.H., and A.G.V. discussed the interpretation of the results; A.G.V. and F.B. wrote the initial draft of the manuscript; H.-W.H. and A.G. contributed to its final version.

Funding

Open Access funding enabled and organized by Projekt DEAL.

Competing interests

The authors declare no competing interests.

Additional information

Supplementary information The online version contains supplementary material available at https://doi.org/10.1038/s42005-023-01281-2.

Correspondence and requests for materials should be addressed to Fabian Brauneis or Artem G. Volosniev.

Peer review information *Communications Physics* thanks the anonymous reviewers for their contribution to the peer review of this work. A peer review file is available.